

1 **The isotopic record of Northern Hemisphere atmospheric carbon monoxide**
2 **since 1950; implications for the CO budget – Supplementary Material**

3 Z. Wang¹, J. Chappellaz², P. Martinerie², K. Park^{1*}, V. Petrenko^{3,**}, E. Witrant⁴, L. K. Emmons⁵,
4 T. Blunier⁶, C. A. M. Brenninkmeijer⁷, J. E. Mak¹

5 ¹Institute for Terrestrial and Planetary Atmospheres/School of Marine and Atmospheric
6 Sciences, Stony Brook University, Stony Brook, NY 11794, USA

7 ²UJF – Grenoble 1 / CNRS, Laboratoire de Glaciologie et Géophysique de l'Environnement
8 (LGGE) UMR 5183, Grenoble, F-38041, France

9 ³Institute of Arctic and Alpine Research, University of Colorado, Boulder, CO 80309, USA

10 ⁴Grenoble Image Parole Signal Automatique (GIPSA-lab), Université Joseph Fourier/CNRS, BP
11 46, 38 402 Saint Martin d'Hères, France

12 ⁵National Center for Atmospheric Research, Atmospheric Chemistry Division, Boulder CO
13 80301, USA

14 ⁶Centre for Ice and Climate, Niels Bohr Institute, University of Copenhagen, Juliane Maries vej
15 30, 2100 Copenhagen Ø, Denmark

16 ⁷Max Planck Institute for Chemistry, 55128 Mainz, Germany

17 * now at: Division of Polar Climate Research, Korea Polar Research Institute, Incheon, South
18 Korea

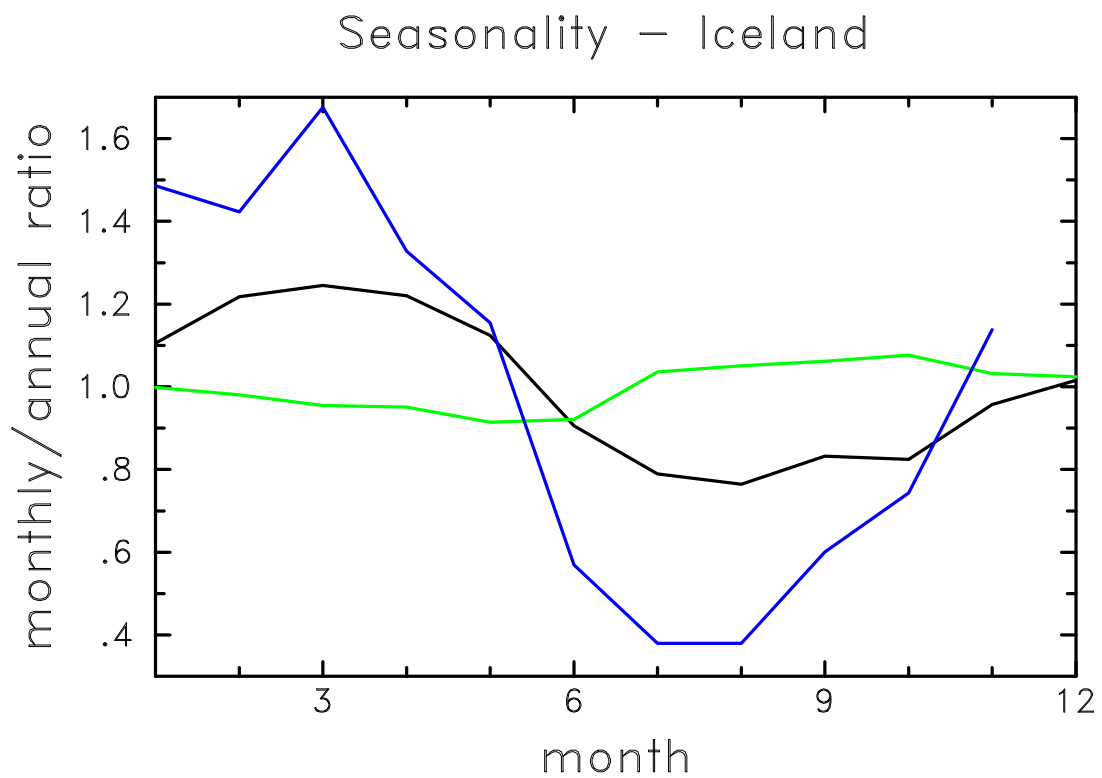
19 ** now at: Department of Earth and Environmental Sciences, University of Rochester, Rochester,
20 NY, USA

21 Correspondence to: Z. Wang (zhihui.wang@stonybrook.edu)

22

23 This document serves as a supplement to ‘The isotopic record of Northern Hemisphere
24 atmospheric carbon monoxide since 1950; implications for the CO budget’. It consists of four
25 figures, one table, and some text, which provide additional modeling results that were omitted in
26 the main article in order to improve its readability.

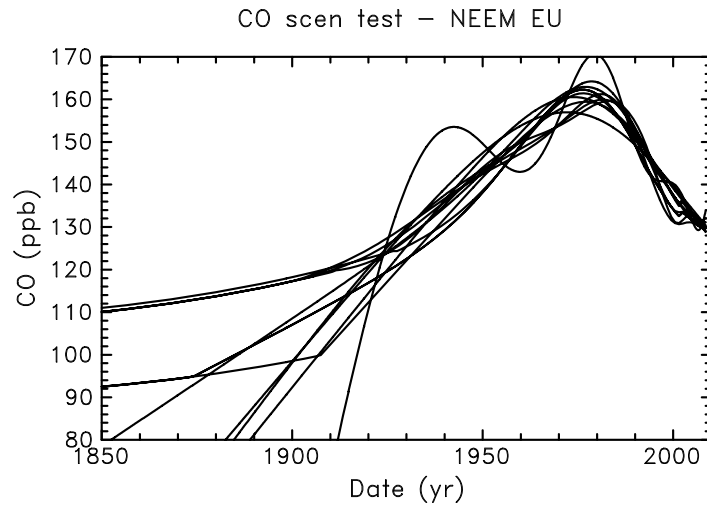
27



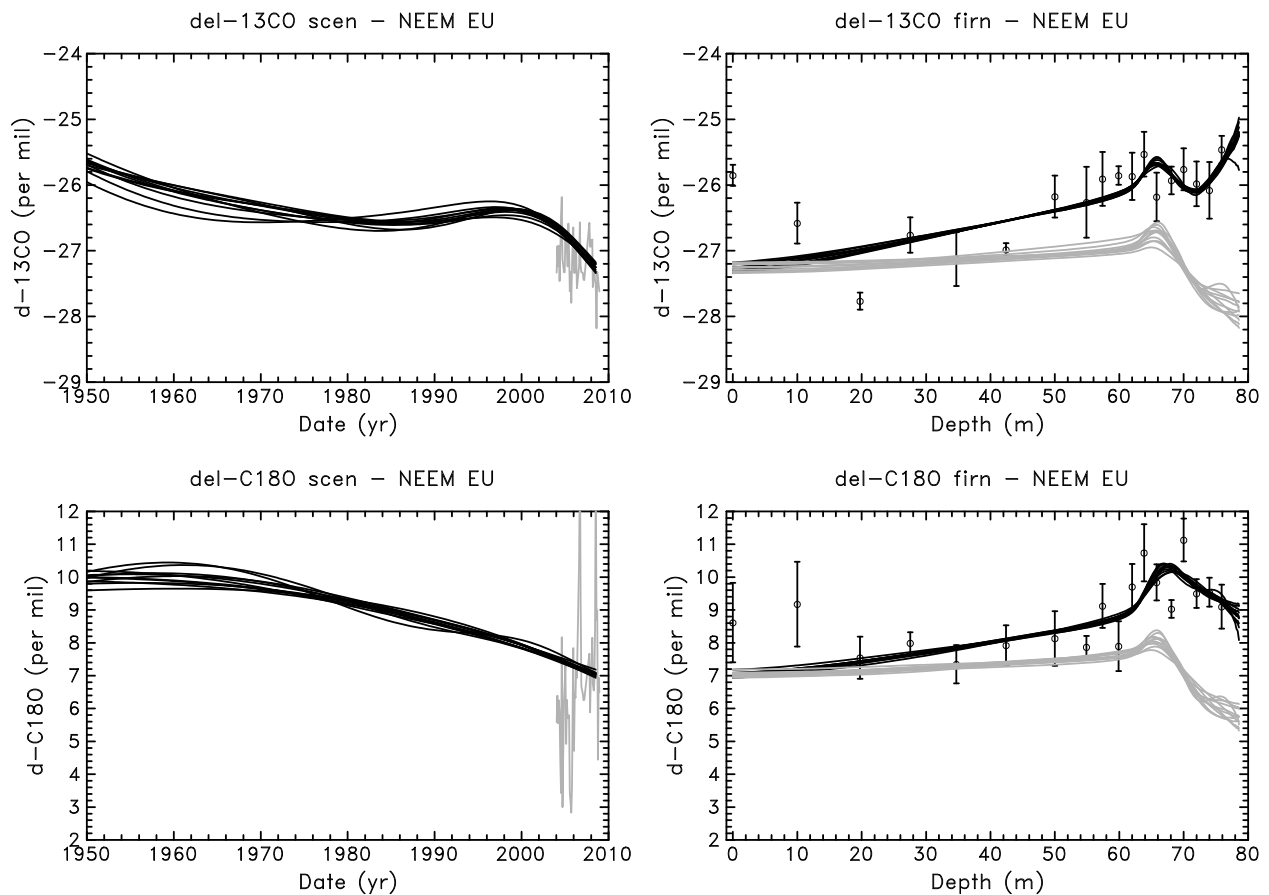
28

29 Fig. S1. Mean seasonality of CO (in black), $\delta^{13}\text{C}$ (in green) and $\delta^{18}\text{O}$ (in blue) of CO in Iceland
 30 expressed a relative values: monthly mean value divided by annual mean value (Wang et al.,
 31 2012).

32



33



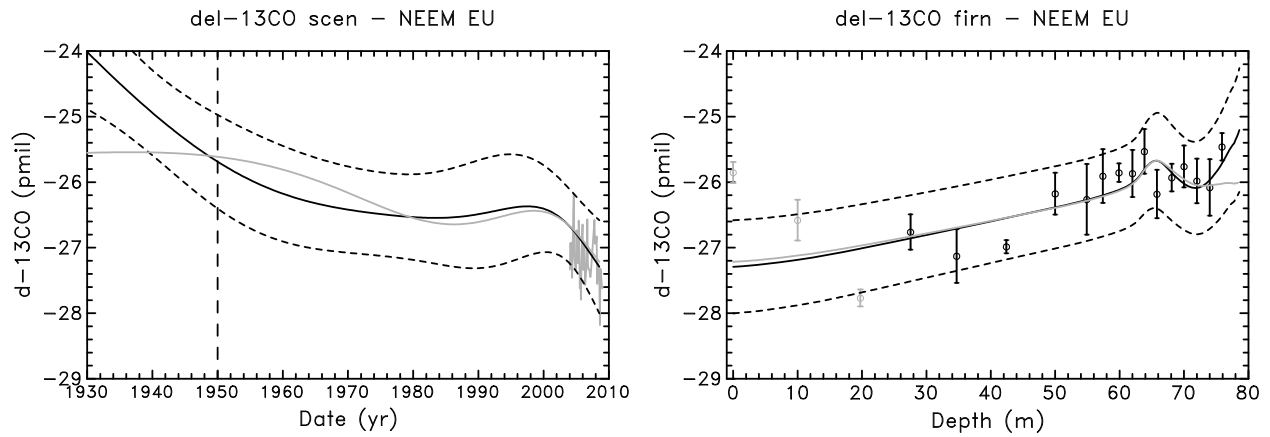
34

35 Fig. S2. Estimation of the effect of the CO trend uncertainty on CO isotopes trend
 36 reconstructions. Upper panel: CO scenarios used for the uncertainty test. Medium panel:
 37 reconstructed $\delta^{13}\text{C}$ trends (left) and their matching of firn data in black (right); the grey curves in
 38 left panel show the recent de-seasonalized isotopic trend in Iceland ; the grey curves in right

39 panel show the effect of CO trends with a constant atmospheric $\delta^{13}\text{C}$. Lower panel: same as
40 medium panel for $\delta^{18}\text{O}$.

41

42
43



44

45 Fig. S3. Influence of removing the deepest measurement of $\delta^{13}\text{C}$ from the dataset used for the
46 atmospheric trend reconstruction. The black lines show the best estimates. The grey lines show
47 the result of a simulation that does not use the deepest $\delta^{13}\text{C}$ measurement as a constraint. Results
48 are shown prior to 1950 in order to visualize the effect of this test on the un-constrained part of
49 the scenario (see section 4.5).

50

51 Discussion on atmospheric trend of $\delta^{13}\text{C}$

52 Figure S2 shows a $\sim 1.4\%$ decrease in $\delta^{13}\text{C}$ between 1950 and 2008. Based on the mean values of
53 $[\text{CO}]$ (Fig. 3), $[\text{CO}]$ source contributions (Fig. 5 and 6) and the $\delta^{13}\text{C}$ isotopic signature at Iceland
54 (Table S1), the mass balance calculation can be performed with the following equation:

55
$$\delta^{13}\text{C} = \sum_{i=1}^7 [\text{CO}_i]/[\text{CO}] \times \delta^{13}\text{C}_i \quad (1)$$

56 where $\delta^{13}\text{C}$ is the calculated $\delta^{13}\text{C}$ and i denotes an individual CO source: fossil fuel
57 combustion, methane oxidation, NMHC oxidation, biofuel burning, biomass burning, direct
58 biogenic, and oceanic emission. $[\text{CO}_i]$ stands for CO concentration from each source calculated
59 from $[\text{CO}]$ and the $\delta^{18}\text{O}$ based mass balance model (Fig. 5 and 6) and $[\text{CO}]$ is the atmospheric
60 CO concentration derived from Greenland firm air measurements and firm model simulations
61 (Petrenko et al., 2012). $\delta^{13}\text{C}_i$ is the $\delta^{13}\text{C}$ source signature at high northern latitudes (Table S1).
62 The results of calculated $\delta^{13}\text{C}$ in 1950-2008 are shown in Fig. S4. The $\delta^{13}\text{C}$ source signatures
63 used here are listed in Table S1. We perform tests with mean CO source contributions and with
64 corresponding uncertainties of CO source contributions. The upper limit and lower limit of
65 calculated $\delta^{13}\text{C}$ is shown in Fig. S4.

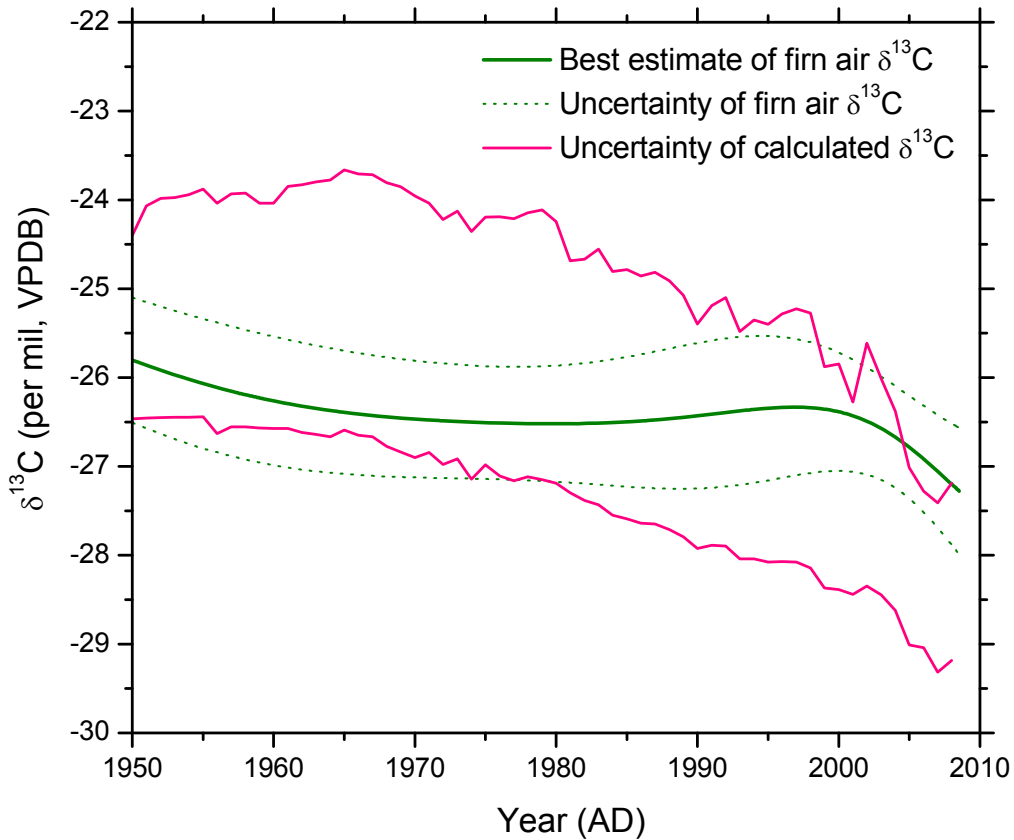
66 The uncertainties of CO source contributions from our mass balance model and $\delta^{13}\text{C}$ source
67 signature contribute to the uncertainties of calculated $\delta^{13}\text{C}$ values. Even though large
68 uncertainties of calculated $\delta^{13}\text{C}$ values are obtained, the observation based firm air $\delta^{13}\text{C}$ (green
69 lines) roughly falls within the range of the calculated $\delta^{13}\text{C}$ (pink lines) (Fig. S4). We do not
70 expect that the calculated $\delta^{13}\text{C}$ trend perfectly reproduces the firm air $\delta^{13}\text{C}$ trend. We do this
71 comparison in order to see if the calculated $\delta^{13}\text{C}$ trend between 1950 and 2008 is significantly
72 different from the observation based firm $\delta^{13}\text{C}$ trend. It has to be pointed out that we have more

73 confidence on the observation based firn air $\delta^{13}\text{C}$ trend than on the calculated $\delta^{13}\text{C}$ since our
74 mass balance calculation involve important assumptions (e.g. steady state assumption and
75 constant OH). We present here the most-likely scenarios of calculated $\delta^{13}\text{C}$ trend based on the
76 data, which are still very valuable.

77 Table S1. MOZART-4 simulations on atmospheric CO at Iceland in 1997-2004^(a)

Sources	Estimated $\delta^{13}\text{C}$ at Iceland (‰) ^(b)
Fossil fuel	-24
Methane oxidation	-49
NMHC oxidation ^(b)	-15
Biofuel ^(c)	-21
Biomass burning ^(d)	-8 to -20
Biogenic	-26
Ocean	-23

78 ^(a): Data in the table is based on MOZART-4 simulation and original $\delta^{13}\text{C}$ source signatures
 79 (Manning et al., 1997 and references therein). (b): assume a constant source signature for the
 80 period 1950-2008. (d): assume C3/C4 plant ratio of burned biomass is between 1:9 and 9:1.



81

82 Fig. S4. Comparison of calculated $\delta^{13}\text{C}$ from mass balance calculation and the estimated $\delta^{13}\text{C}$ in
 83 NEEM firn air by LGGE-GIPSA models. Green solid line and dotted lines are the same as those
 84 in Fig. 4. Pink lines are uncertainties of calculated $\delta^{13}\text{C}$ derived from all the uncertainties (see
 85 text).

86

87

88 **References**

89 Manning, M. R., Brenninkmeijer, C. A. M., and Allan, W.: Atmospheric carbon monoxide
 90 budget of the southern hemisphere: Implications of $^{13}\text{C}/^{12}\text{C}$ measurements, *Journal of*
 91 *Geophysical Research-Atmospheres*, 102, 10673-10682, 1997.
 92 Petrenko, V., Martinerie, P., Novelli, P., Etheridge, D. M., Levin, I., Wang, Z., Petron, G.,
 93 Blunier, T., Chappellaz, J., Kaiser, J., Lang, P., Steele, L. P., Vogel, F., Leist, M. A., Mak, J.,
 94 Langenfelds, R. L., Schwander, J., Severinghaus, J. P., Forster, G., Sturges, W., Rubino, M.,
 95 and White, J. W. C.: Records of Northern Hemisphere carbon monoxide and hydrogen back
 96 to ~1950 from Greenland firn air, *Atmospheric Chemistry and Physics*, in preparation, 2012.
 97 Wang, Z., Park, K., Emmons, L., and Mak, J. E.: Interannual variations of anthropogenic source
 98 of atmospheric CO at high northern latitudes during 2004-2009. In preparation., 2012.